BMP10 is essential for maintaining cardiac growth during murine cardiogenesis

Hanying Chen[1], Shu Shi[1], Lourdes Acosta[2], Weiming Li[1], Jonathan Lu[3], Shideng Bao[4], Zhuang Chen[1], Zuocheng Yang[1], Michael D. Schneider[5], Kenneth R. Chien[3], Simon J. Conway[1], Mervin C. Yoder[1], Laura S. Haneline[1], Diego Franco[2] and Weinian Shou[1,*]

[1]Herman B Wells Center for Pediatric Research, Department of Pediatrics, Indiana University School of Medicine, Indianapolis, IN 46202, USA
[2]Department of Experimental Biology, University of Jaen, Jaen 23071, Spain
[3]Department of Medicine, University of California San Diego, La Jolla, CA 92093, USA
[4]Department of Pharmacology and Cancer Biology, Duke University Medical Center, Durham, NC 27708, USA
[5]Department of Medicine, Baylor College of Medicine, Houston, TX 77030, USA
*Author for correspondence (e-mail: wshou@iupui.edu)

Accepted 7 January 2004

Development 131, 2219-2231
Published by The Company of Biologists 2004
doi:10.1242/dev.01094

Summary

During cardiogenesis, perturbation of a key transition at mid-gestation from cardiac patterning to cardiac growth and chamber maturation often leads to diverse types of congenital heart disease, such as ventricular septal defect (VSD), myocardium noncompaction, and ventricular hypertrabeculation. This transition, which occurs at embryonic day (E) 9.0-9.5 in murine embryos and E24-28 in human embryos, is crucial for the developing heart to maintain normal cardiac growth and function in response to an increasing hemodynamic load. Although, ventricular trabeculation and compaction are key morphogenetic events associated with this transition, the molecular and cellular mechanisms are currently unclear. Initially, cardiac restricted cytokine bone morphogenetic protein 10 (BMP10) was identified as being upregulated in hypertrabeculated hearts from mutant embryos deficient in FK506 binding protein 12 (FKBP12). To determine the biological function of BMP10 during cardiac development, we generated BMP10-deficient mice. Here we describe an essential role of BMP10 in regulating cardiac growth and chamber maturation. BMP10 null mice display ectopic and elevated expression of $p57^{kip2}$ and a dramatic reduction in proliferative activity in cardiomyocytes at E9.0-E9.5. BMP10 is also required for maintaining normal expression levels of several key cardiogenic factors (e.g. NKX2.5 and MEF2C) in the developing myocardium at mid-gestation. Furthermore, BMP10-conditioned medium is able to rescue BMP10-deficient hearts in culture. Our data suggest an important pathway that involves a genetic interaction between BMP10, cell cycle regulatory proteins and several major cardiac transcription factors in orchestrating this transition in cardiogenesis at mid-gestation. This may provide an underlying mechanism for understanding the pathogenesis of both structural and functional congenital heart defects.

Key words: BMP10, $p57^{kip2}$, NKX2.5, MEF2C, Cardiac growth, Ventricular trabeculation, Compaction

Introduction

Cardiac development is a complex and sequential process that is composed of a series of morphogenetic events, such as cardiogenic induction and patterning, cardiomyocyte growth and differentiation, multiple cell lineage specification, and terminal differentiation and chamber maturation (for a review, see Srivastava and Olson, 2000). These events are regulated by cardiogenic transcriptional factors and growth/differentiation factors. Genetic mutations of these genes lead to either early embryonic lethality or a vast majority of congenital heart defects (CHDs) that affect 1/200 live births. One of many forms of CHD is ventricular noncompaction, or spongy myocardium, which is based on its characteristic feature of abnormal ventricular myocardium with hypertrabeculation and noncompaction (Dusek et al., 1975; Ichida et al., 2001). It is a unique type of cardiomyopathy generally found in infant patients. These patients may proceed to have dilated hearts and congestive heart failure. Commonly associated defects are ventricular septal defect (VSD) and pulmonic stenosis (PS). This noncompaction of ventricular myocardium has been defined as a morphogenetic abnormality and is clearly due to defects in the ventricular trabeculation and compaction.

Ventricular trabeculation and compaction are important morphogenetic processes and are closely associated with cardiac growth regulation at mid-gestation (Rumyantsev, 1991; Icardo, 1984). At the final stage of cardiac looping (E9.0-E9.5), initially the endocardium penetrates through the cardiac jelly and evaginates at discrete points of myocardium to form ‘outpockets’ directed toward the myocardium. These endocardium outpockets initiate the cardiac trabeculation. Further expansion of primitive trabecular myocardium between E9.5 and E13.5, via either myocyte recruitment or proliferation, is an important step in generating matured trabeculae. Later in development (E14.5-E15.5), trabecular

myocytes in the developing myocardium undergo 'compaction' and gradually become part of compact wall, papillary muscles, interventricular septum and conductive system cells (Moorman and Lamers, 1999), respectively. One of the scientific challenges is to determine the molecular mechanism by which cardiac trabeculation and subsequent compaction are regulated. Several endocardial growth factors required for the development of trabeculae, such as neuregulin (Meyer and Birchmeier, 1995) and its receptors ErbB (Gassmann et al., 1995; Lee et al., 1995), vascular endothelial growth factor (VEGF) (Ferrara et al., 1996), and angiopoietin-1 (Suri et al., 1996), have been identified. Mutant mice deficient in these genes have severe defects in ventricular trabeculation. However, more detailed analysis is still required to determine their precise role in the process of ventricular trabeculation and compaction.

Bone morphogenetic proteins (BMPs), named for their initial biological activity of inducing ectopic bone formation, belong to the transforming growth factor β (TGFβ) superfamily. They mediate a diverse spectrum of developmental events throughout evolution in species ranging between insects and mammals (for a review, see Ducy and Karsenty, 2000; Nakayama et al., 2000). BMP signals have been shown to link multiple steps of cardiac development, including cardiogenic induction and endocardial cushion formation (for a review, see Schneider et al., 2003). Unlike other BMPs, BMP10 expression is restricted to the developing and postnatal heart (Neuhaus et al., 1999). The most interesting feature of BMP10 is its transient presence in the developing trabecular myocardium. In this study, we found that BMP10 was upregulated in trabecular myocardium of genetically manipulated mutant mice deficient in FK506 binding protein 12 (FKBP12) (Shou et al., 1998). FKBP12 is able to bind type I receptors for BMP/Activin/TGFβ and possibly plays a role in preventing premature activation of type I receptors (Wang et al., 1994; Wang et al., 1996) (for a review, see Massague and Chen, 2000). FKBP12-defcient mice are embryonically lethal due to enormous overproduction of ventricular trabeculae, which severely impairs cardiac development and function. In this study, we generated BMP10-deficient mice and analyzed the biological function of BMP10 during cardiac trabeculation and uncovered a BMP10-mediated molecular pathway essential for regulating cardiac growth and function at mid-gestation.

Materials and methods

RNA differential display and molecular cloning of BMP10

The PCR-based RNA differential display was based on the previously described protocol (Bao et al., 1998). Briefly, cellular mRNA samples were isolated from pooled FKBP12-deficient and littermate control E14.5 embryonic cardiac tissues, respectively. S^{35}-labeled cDNA fragments were amplified by PCR using a set of palindromic primers and rTh DNA polymerase and Mn^{2+} and Mg^{2+} reaction buffer system (Perkin Elmer Cetus). The differentially expressed gene products revealed by the mRNA display were confirmed by Northern blot before being processed for sequencing. The mouse BMP10 full-length cDNA was obtained by RT-PCR and was confirmed by sequencing.

RT-PCR reactions

MicroPoly(A)Pure kit (Ambion) was used to isolate mRNA from mouse embryos or pooled embryonic hearts. The first-strand synthesis and PCR reaction were performed using RETROscript kit (Ambion) according to the manufacturer's instructions. The sets of primers are: 5′ BMP10 primer, ACCAGACGTTGGCAAAAGTCAGGC; 3′ BMP10 primer, GATGATCCAGGAGTCCCACCCAAT; 5′ $p57^{kip2}$ primer, AGTCTGTGCCCGCCTTCTAC; 3′ $p57^{kip2}$ primer, CTCAGTTCCCAGCTCATCACCC; 5′ FKBP12 primer, CACGTGGATCTGCCATGGAGGAA; 3′ FKBP12 primer, GTGGAAGGACTGACAGAAGCCAA; 5′ GAPDH primer, GGGTGGAGCCAAACGGGTC; 3′ GAPDH primer, GGAGTTGCTGTTGAAGTCGCA.

Targeted deletion and generation of BMP10-deficient mice

A BMP10 genomic clone was isolated from a mouse 129SvEv genomic BAC library (RPCI-22 129 mouse library from BAC/PAC Resources, Children's Hospital Oakland). The mouse BMP10 gene contains two exons (Fig. 3A). Linearized targeting vector (25 μg) was electroporated into embryonic stem (ES) cells (CCE916 ES cell line), clones were selected in G418 and gancyclovir, DNA from the clones was analyzed by Southern blot, and targeted ES cell lines BMP10-B12 and BMP10-F8 were expanded and injected into blastocysts. Male chimeras were bred to C57BL/6J or 129SvEv females to generate F1 offspring. Mutant mice generated from both targeted ES cell lines had identical phenotype.

Histological, morphological, ink injection, whole-mount and section in-situ hybridization, and immunohistochemistry analyses

Embryos were harvested by cesarean section. Embryos and isolated hearts were fixed in 10% neutral buffered formalin, paraffin embedded, and sectioned (6 μm), and stained with hematoxylin and eosin. To analyze the proliferative activity of the developing heart, timed-mated females were given a single injection of tritiated thymidine (200 μCi ip at 28 Ci/mM; Amersham Biosciences Corp.). Embryos were harvested after a 3-hour labeling period, and followed by fixation (10% neutral buffered Formalin) and paraffin sectioning. Deparaffined sections were stained with Hoechst in PBS to identify the cell nucleus. The Hoechst-stained slides were coated with photographic emulsion (Polysciences, Warrington, PA, USA) and further processed for autoradiography. [^{3}H]thymidine labeling index was the percent of labeled nuclei versus the total number of nuclei. Ink-injection analysis was performed as previously described (Winnier et al., 1999). Both whole-mount and section in-situ hybridization were performed as previously described (Franco et al., 2001). Complementary RNA probes of various cardiac markers were labeled with digoxingenin-UTP using Roche DIG RNA Labeling system according to the manufacturer's guidelines. HOP probe was a generous gift of Dr Epstein (Chen et al., 2002). These probes were hybridized with paraformaldehyde-fixed embryos or hearts for whole-mount in-situ staining or with either frozen or deparaffined sectioned samples for in-situ staining. To analyze $p57^{kip2}$ expression in the heart, we used a monoclonal antibody against mouse $p57^{kip2}$ (Labvision, ms-897-P1) and a Vector staining system (Vector, PK-2200) according to the manufacturer's instructions.

Whole-mount immunostaining and confocal microscopic imaging

Embryos were washed three times in PBS and fixed for 10 minutes in pre-chilled acetone before being treated with blocking solution containing 3% non-fat dry milk (Bio-Rad Laboratories, Hercules, CA) and 0.025% Triton X-100 for 1 hour. Directly conjugated primary antibodies were then added to a final concentration of 1 μg/ml for 12 to 18 hours at 4°C. Anti-Flk-1 (PharMingen, San Diego, CA) and MF-20 monoclonal antibodies (Hybridoma bank, University of Iowa) were labeled with Alexa Fluor 488 and Alexa Fluor 647, respectively, using a monoclonal antibody labeling kit (Molecular Probes, Eugene, OR). Samples were analyzed using a Bio-Rad MRC 1024 Laser Scanning Confocal Microscope (Bio-Rad Microscopy Division, Cambridge, MA) equipped with a Krypton-Argon laser (488, 647 nm). 3D series

(Z series) were obtained by imaging serial confocal planes at 512×512 pixel resolution with a Nikon 20X oil-immersion objective (2 μm intervals).

Generation of BMP10 expressing NIH3T3 cells

The coding region of the mouse BMP10 cDNA was subcloned into 5′ of an IRES-EGFP cassette in the retroviral vector MIEG3. Ecotropic packaging cell lines were established for MIEG3-BMP10 and MIEG3 vector control as described (Haneline et al., 2003). NIH3T3 cells were transduced with retroviral supernatants (containing approximately 1×10^5 viral particles/ml) in a similar way to previously published methods (Haneline et al., 2003). Transduced cells were kept in DMEM containing 10% FBS for 3 days before sorting for EGFP positive cells using FACSVantage SE (Becton Dickinson). Northern blot analysis confirmed that the BMP10 transcript was detected only in NIH3T3 cells transduced with MIEG3-BMP10 (NIH3T3/BMP10) and not in cells transduced with vector control (NIH3T3/EGFP).

Cardiomyocyte-NIH3T3 cell co-culture to assay the proliferative activity of cardiomyocytes

NIH3T3/BMP10 and NIH3T3/EGFP cells were used as feeders in our cardiomyocyte co-culture assay. We first treated feeder cells with mitomycin C (10 μg/ml) for 2 hours to prevent proliferation. After washing twice in PBS, mitomycin C-treated cells were trypsinized and re-suspended in DMEM containing 2% FBS and were mixed with freshly isolated mouse embryonic cardiomyocytes (E12.5). Cells were plated on one-well Lab-Tek chamber slides. The final plating density was $2\text{-}3\times10^5$ total cells for each well. Cells were labeled with [^{3}H]thymidine for 2 hours and fixed in methanol and processed for autoradiography and Periodic Acid-Schiff (PAS) staining. The DNA-[^{3}H]thymidine labeling index of PAS positive cells (cardiomyocytes) was recorded and compared between experimental and control groups.

Culture of isolated embryonic hearts

Based on the method previously described (Conway et al., 1997; Rentschler et al., 2002), embryonic hearts were dissected from E9.25 or E9.5 embryos in DMEM containing 10% FBS, and washed twice in PBS and cultured for 8, 12 or 24 hours in BMP10-conditioned or control media. BMP10-conditioned media were collected from overnight culture of BMP10 expressing cells (NIH3T3/BMP10). Control media were collected from overnight culture of control cells (NIH3T3/EGFP). Both BMP10-conditioned and control media were derived from DMEM containing 1% FBS. Conditioned media for BMP-2, -4, -5, -6 and TGFβ-1 (final concentration: 50 ng/ml) and neuregulin (NRG-1, final concentration: 2.5×10^{-9} M) were prepared by adding each activated growth factors to DMEM containing 1% serum right before the culture to reach the final concentration (Barron et al., 2000; Rentschler et al., 2002). BMP-2, -4, -5, -6 and TGFβ-1 were from Sigma. NRG-1 was from R & D Systems.

Results

BMP10 is upregulated in hypertrabeculated hearts deficient in FKBP12

FKBP12-deficient mice develop severe cardiac defects with the unique phenotype of hypertrabeculation and noncompaction (Shou et al., 1998), suggesting that the FKBP12-deficient mouse is a valuable mouse model to study the molecular mechanism of cardiac trabeculation. To screen for candidate genes that were abnormally expressed in FKBP12-deficient hearts, specifically in overproduced trabecular myocardium, we used RNA differential display. RNAs were isolated from pooled E14.5 hearts of FKBP12-deficient and control embryos. RNA differential displays (data not shown) were performed as previously described (Bao et al., 1998). BMP10 was identified in this gene profiling study. BMP10 expression was significantly elevated in FKBP12-deficient hearts, as confirmed by northern blot analysis (Fig. 1A, part k).

BMP10 expression in developing and adult heart

We carefully analyzed the expression pattern of BMP10 in developing and adult mouse hearts using whole-mount and section in-situ hybridization analyses (Fig. 1A, parts a-i). During cardiac development, BMP10 is expressed transiently in the ventricular trabecular myocardium from E9.0-13.5, a critical time span when cardiac development shifts from patterning to growth and chamber maturation (Fig. 1A, parts b,c,e-h). Using RT-PCR, we could detect BMP10 expression as early as E8.75, but not in E16.5 ventricles (Fig. 1A, part j). By E16.5-E18.5, BMP10 was only detectable in atria (Fig. 1A, parts d,j). This finding is consistent with previously published work (Neuhaus et al., 1999). Interestingly, in adult hearts BMP10 was present in the right atrium but not in the left atrium (Fig. 1A, part i), which was further confirmed by a quantitative RNA analysis using Clontech adult tissue mRNA array (Fig. 1B).

Generation of BMP10-deficient mice

The mouse BMP10 gene contains only two exons. The second exon encodes a proteolytic processing site and the mature peptide. To generate a null mutation in the mouse BMP10 gene, we deleted most of the coding region (*bmp10*^{m1}) using mouse embryonic stem cell technology (Fig. 2A). Genomic Southern blot using 3′-probe (Fig. 2B) and PCR analyses were used to genotype targeted ES cells and mutant mice. RT-PCR was used to confirm that BMP10 expression was absent in BMP10-deficient embryos (Fig. 2C).

Heterozygous (*bmp10*^{m1}/+) mice were viable and fertile and were intercrossed to obtain homozygous (*bmp10*^{m1}/*bmp10*^{m1}) mutants. Genotyping analysis of 191 F_2 129SvEv inbred and 230 F_2 C57BL6/129SvEv hybrid offspring at weaning demonstrated no viable BMP10-deficient mice. The distribution of genotypes in E9.5 embryos (105 wild-type [24%], 244 heterozygotes [56%], and 87 homozygotes [20%]) and in E10.5 embryos (95 wild-type [30%], 190 heterozygotes [61%], and 28 homozygotes [9%]) suggested that BMP10-deficient mice were dying in utero between E9.5 and E10.5.

Embryonic lethality of BMP10-deficient mice is due to severely impaired cardiac development and function

We carried out morphological and histological analyses on embryos from E8.5 to E10.5 (Fig. 3A). At E8.5-8.75 (8-12 somite pair stage), BMP10-deficient embryos appeared normal compared to wild-type and heterozygous littermate controls, suggesting that BMP10 was not required for cardiac patterning (Fig. 3A, parts a-d). At E9.0-E9.5 (15-20 somite pair stage), while having normal pairs of somites in mutant embryos, normal allantoic/umbilical connection, and normal vasculature development in mutant yolk sacs and embryos, cardiogenesis appeared arrested in BMP10-deficient embryos (Fig. 3A, parts e-p). These mutant embryos displayed cardiac dysgenesis with profound hypoplastic ventricular walls and absence of ventricular trabeculae. The development of endocardial cushions was abnormal in both outflow track (OFT) and atrial-ventricular canal (AVC) and was halted at the acellular stage.

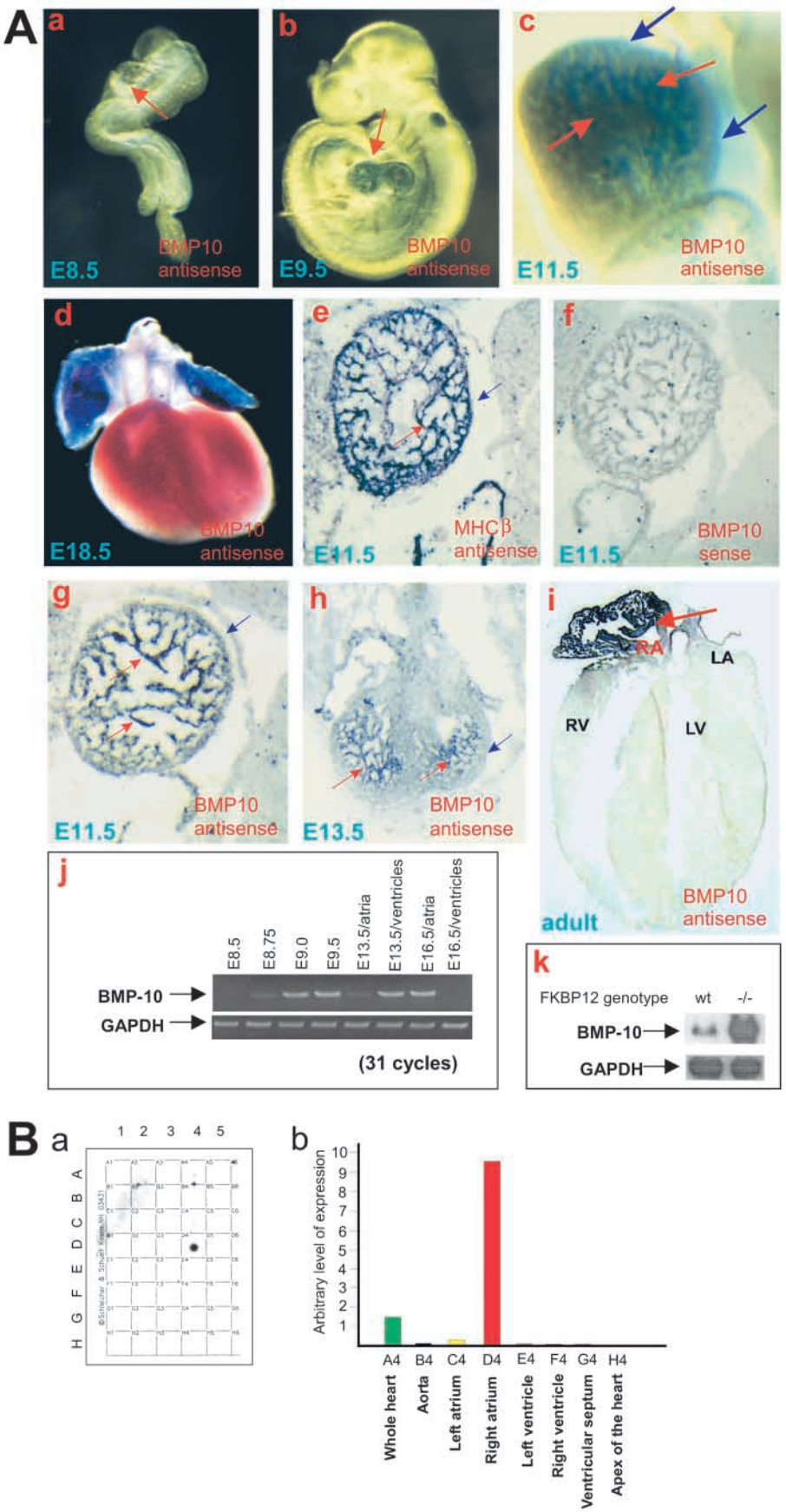

Fig. 1. Expression pattern of BMP10 during cardiogenesis. (A) In (a-d), using whole-mount in-situ hybridization, BMP10 transcripts were not detected in E8.5 embryonic hearts (a), but were detected in developing ventricles and atria at E9.5 (b), and at E11.5 (c). BMP10 expression was restricted to trabecular myocardium. Red arrows indicate the heart in (a,b) and trabecular myocardium in (c), and blue arrows indicate the ventricular compact wall. (d) BMP10 expression was detected only in atria at E18.5. In (e-i), in-situ hybridizations were performed on sagittal sections of E11.5, transverse sections of E13.5 embryos, and transverse sections of an adult mouse heart. (e) Myosin heavy chain β (MHCβ) transcripts were detected throughout the myocardium. (f) A BMP10 sense probe was used as a negative control. (g,h) BMP10 expression in the ventricle was restricted to trabecular myocardium and (i) became restricted to the right atrium in adults. (j) BMP10 transcripts were detected in the heart as early as E8.75 using RT-PCR. By E16.5, BMP10 was hardly detectable in ventricles. (k) Using northern blot to confirm BMP10 expression in FKBP12-deficient hearts (E14.5). BMP10 transcripts were significantly upregulated in FKBP12-deficient hearts. (B) Multiple-tissue quantitative mRNA level analysis. (a) Quantitative dot blot analysis of evenly loaded 84 mRNA samples from varying adult human tissues (Clontech). Only mRNA samples isolated from whole heart (A4) and right atrium (D4) showed significant BMP10 mRNA level when compared to negative control samples. (b) Phosphorimage analysis on the relative level of expression of BMP10 in different regions of the adult heart. The phosphorimaging values were corrected for the mean background, consisting of negative controls (yeast total RNA, yeast tRNA, *E. coli* rRNA, *E. coli* DNA) and empty fields.

At this developmental stage, BMP10-deficient hearts exhibit rhythmic contraction, but at a significantly slower rate compared with littermate controls [43±6 beats/minute in mutant hearts (n=12) versus 96±7 beats/minute in wild-type and heterozygous littermate controls (n=15), P<0.0001]. To visualize and compare the cardiac function and circulation in mutants and controls, ink was injected into the primitive left ventricle of E9.0 and E9.5-9.75 embryos. As shown in Fig. 3B, while circulation was established in BMP10 mutant embryos at E9.0, severely impaired cardiac function and circulation was observed in mutant embryos at E9.5-9.75. By E10.0-E10.5, mutant embryos appeared to be dying (Fig. 3A, parts q-t).

The outgrowth of ventricular trabecular myocardium is defective in the BMP10-deficient heart

It has been suggested that cardiac trabeculation is the consequence of interactions between the developing myocardium and the 'outpocketing' endocardium at E9.0-E9.5 (Icardo, 1984). To better understand if the lack of ventricular trabeculae in the BMP10-deficient heart was due to the failure of endocardial outpocketing (i.e. initiation of trabeculation) or the failure of a myocardial response (i.e. further expansion of trabecular myocardium through either myocyte recruitment or growth), we used confocal microscopy to analyze the structural relationship between endocardium and myocardium in BMP10-deficient hearts at E9.5 (Fig. 4). Endothelial receptors for vascular endothelial growth factor (Flk1) (Millauer et al., 1993) and angiopoietin (Tek/Tie2) (Dumont et al., 1994) (data not shown) were normal in BMP10-deficient endothelial cells throughout the developing cardiovasculature compared with wild-type and heterozygous littermate controls at E9.5 (Fig. 4A,B). MF20 staining (anti-myosin heavy chain) was also maintained in the BMP10-deficient myocardium despite overall hypoplasia (Fig. 4C,D). These observations confirmed that BMP10 was not required for differentiation of either endocardium or myocardium. Furthermore, the developing endocardium was in normal proximity to the ventricular wall and the primitive ventricular trabeculae were indeed formed in the BMP10 mutants (Fig. 4C,D). These findings strongly suggested that BMP10 was not crucial to the initiation of cardiac trabeculation, nor myocyte recruitment, but was essential to the further growth of both ventricular wall and trabeculae.

Growth deficiency and ectopic expression of P57^{kip2} in BMP10-deficient myocardium

Surprisingly, TUNEL assays showed no significant cellular apoptosis in E9.5 BMP10 mutant hearts, despite a severely thinned ventricular wall (data not shown). This finding suggested that a defect in myocyte proliferation was the main reason for the hypoplastic wall seen in BMP10-deficient hearts. We used [^{3}H]thymidine labeling to determine the proliferative activity in BMP10-deficient hearts. [^{3}H]thymidine labeling index in the mutant hearts was significantly lower than that in littermate controls (10.1%±2, n=5, in mutants versus 29.0%±3, n=4, in controls, P<0.001). These results further suggested that a marked reduction in proliferation of BMP10-deficient cardiomyocytes was responsible for the hypoplastic ventricular wall and failure of normal ventricular trabeculation.

Among multiple cell cycle regulators, p57^{kip2} expression is first detectable in the developing heart at E10.5 by in-situ hybridization and RT-PCR and is restricted to ventricular trabeculae (Kochilas et al., 1999). Therefore, p57^{kip2} is considered a key negative regulator involved in cardiac cell cycle exit within the developing ventricular trabeculae during chamber maturation (Kochilas et al., 1999). Immunohistochemistry staining revealed that p57^{kip2} was upregulated and ectopically expressed throughout the ventricular wall in BMP10-deficient hearts at E9.5 compared with littermate controls (Fig. 5A, parts a-c). FKBP12-deficient hearts (E13.5), which have elevated BMP10 levels and an overproduction of trabeculae, exhibited significantly lower p57^{kip2} expression in trabecular myocardia compared with littermate controls (Fig. 5A, parts d,e), suggesting a mechanistic

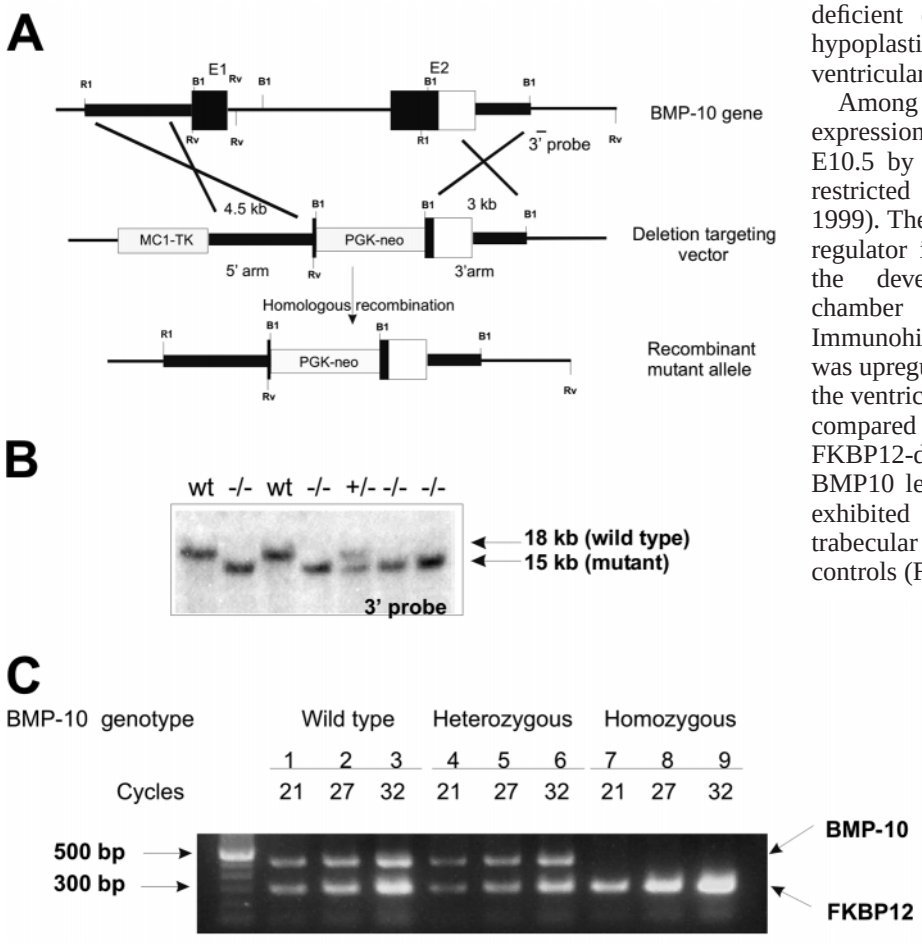

Fig. 2. Generation of BMP10-deficient mice. Targeting vector to mutate the mouse BMP10 gene in embryonic stem cells (a), Southern blot analysis of genomic DNA (digested with EcoRV and probed with 3′-probe) derived from a single litter of E9.5 embryos after mating of *bmp10*^{m1}/+ mice (b), and RT-PCR analysis to confirm the inactivation of BMP10 expression in *bmp10*^{m1}/*bmp10*^{m1} embryos (E9.0) (c). Expression of FKBP12 was used as a loading control.

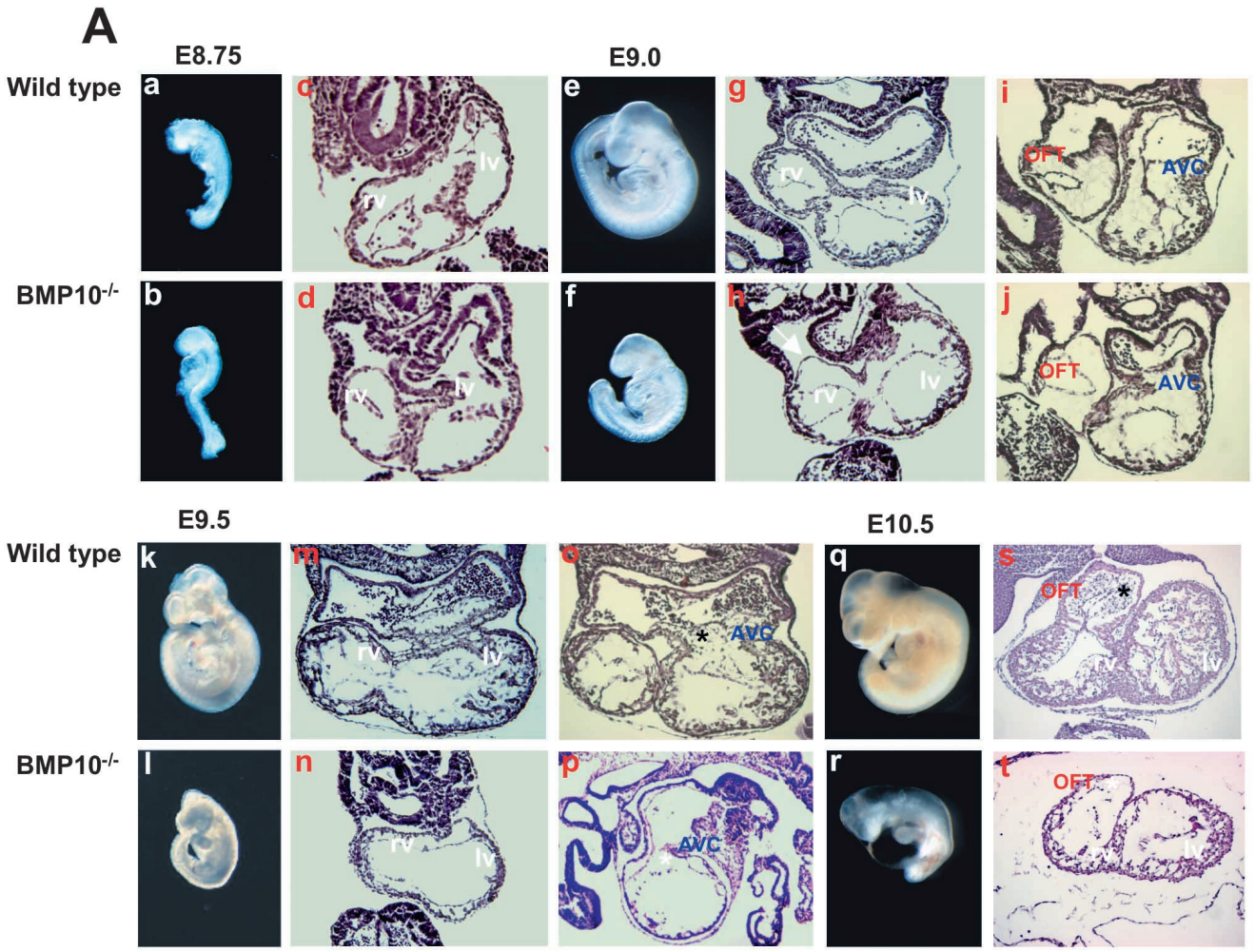

relationship between $p57^{kip2}$ and BMP10. RT-PCR analysis confirmed this observation (Fig. 5B) and further suggested that BMP10 regulated $p57^{kip2}$ at the transcriptional level. Together these data show that elimination or elevation of BMP10 expression jeopardized the regulation of ventricular growth and chamber maturation.

Defects in cardiogenic pathway in BMP10-deficient hearts

To determine if cardiogenic pathways were affected by the loss of BMP10, we evaluated the expression patterns of key cardiac transcriptional factors and chamber-restricted markers. The expression of cardiac chamber-specific markers MLC2v and MLC2a (Franco and Icardo, 2001) were normal in BMP10-deficient hearts at E8.5 (data not shown) and E9.5 (Fig. 6A-D), which further confirmed our observation that BMP10 was not required for cardiac patterning and cardiogenic differentiation. While the expression of cardiogenic transcriptional factors NKX2.5 (Schott et al., 1998) (for a review, see Harvey et al., 1999) and MEF2C (for a review, see Black and Olson, 1999) was normal in BMP10-deficient embryos at E8.5-E8.75 (data not shown), these molecules were dramatically downregulated in the BMP10-deficient hearts at E9.25-E9.5 (Fig. 6E-H). Whole-mount in-

Fig. 3. Morphological and histological analysis of BMP10-deficient embryos and hearts. (A) (a,b,e,f,k,l,q,r) comparison of gross morphology of normal littermate control and BMP10-deficient embryos from E8.75 to E10.5. (a,b) No apparent abnormality was detected at E8.75. (e,f) Some BMP10-deficient embryos were slightly growth retarded at E9.0. (k,l) Severe growth retardation was seen in BMP10-deficient embryos at E9.5; however, mutants had an identical number of somite pairs and normal allantoic connection when compared with littermate controls. Over 50% of BMP10-deficient embryos had severe edema and expanded pericardiac sacs, suggesting poor cardiac function in these mutants. (q,r) BMP10-deficient embryos were dead by E10.5. (c,d,g,h,I,j,m,n,o,p,s,t) comparison of histological sections of normal control and BMP10-deficient hearts from E8.75 to E10.5 embryos stained with haematoxylin and eosin. (d,h,j) At E8.75-E9.0, BMP10-deficient embryos had normal rightward looped heart and primitive ventricular chambers, suggesting that BMP10 is not required for the early phases of cardiogenesis. Also, the size of the heart in BMP10-deficient embryos was grossly normal compared with littermate control but exhibited some thinned myocardium (white arrow). Acellular endocardial cushions were formed in both the outflow track (OFT) and atrial-ventricular canal (AVC). (n,p,t) Compared with wild-type normal hearts at E9.5-E10.5, BMP10-deficient hearts were growth retarded, had hypoplastic walls and failed to develop normal ventricular trabeculae and endocardial cushions. While endocardial cushions in OFT and AVC of wild-type control hearts had begun to be seeded after epithelial-mesenchymal transformation of adjacent endocardium (black asterisks in o and s), acellular endocardial cushions remained in BMP10-deficient hearts (white asterisks). (B) Ink injection was used to visualize the cardiac contractile function and blood flow in E9.0 and E9.5-E9.75 embryos. (a,c) Ink injected in the primitive left ventricle was efficiently pumped throughout the entire cardiovascular system in control embryos. (b) At E9.0, the circulation was established in BMP10-deficient embryos, however, not as efficiently as littermate controls, which might reflect the weaker/slower heart rate in BMP10 mutants. (d) At E9.5-9.75, ink remained in the BMP10-deficient ventricles, suggesting poor cardiac function. Note that the ink within the BMP10-deficient heart has diffused in a retrograde direction into the sinus venous (yellow arrow) and yolk sac (green arrow) due to lack of adequate cardiac contraction and circulation. Red arrows indicate circulated ink around the embryonic head region. Blue arrows indicate hearts. The posterior portions of the embryos were removed to visualize the hearts (c,d).

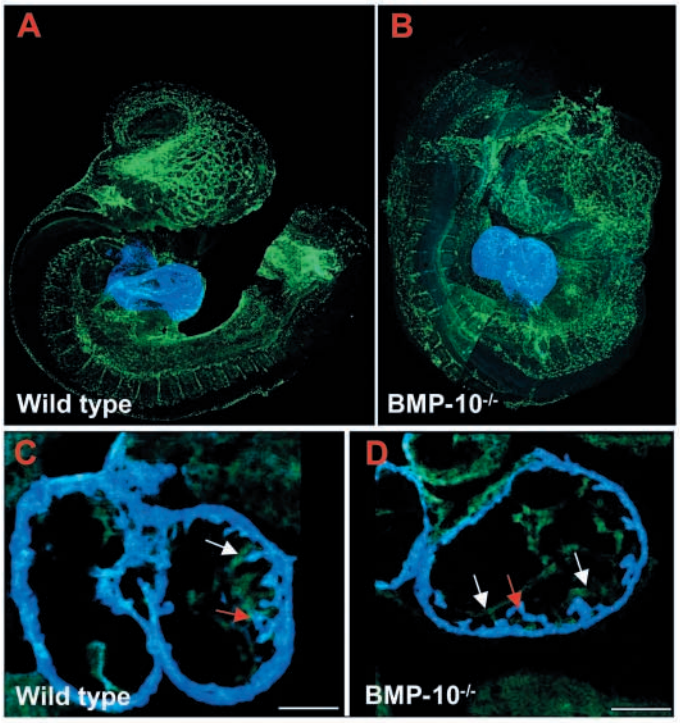

Fig. 4. Whole-mount immunostaining and confocal microscopic analysis of control (A,C) and BMP10-deficient embryos (B,D) at E9.25. Fluorescence conjugated anti-Flk-1 monoclonal antibody stains the endothelial cells (green) in the developing vasculature and endocardium of the developing heart, while anti-myosin heavy chain monoclonal antibody MF-20 stains the myocardium (blue). (A,B) comparison of endothelial development in both control and BMP10-deficient embryos at E9.25. Endothelial development was not affected in BMP10-deficient embryos. (C,D) Comparison of endocardium and myocardium development in control and BMP10-deficient ventricles. The BMP10-deficient heart displayed a much thinner ventricular wall compared with the control heart; however, the endocardium was in normal proximity to the myocardium. Some primitive trabeculae were formed in the BMP10-deficient ventricles at this age. Red arrows point to the primitive trabecular myocardium, while white arrows indicate the endocardium.

situ hybridization revealed that the downregulation of NKX2.5 was restricted to the heart, as NKX2.5 expression in the branchial arches and developing gut remained normal at E9.5 (data not shown). ANF and Chisel are known downstream targets of NKX2.5 (Durocher et al., 1996; Palmer et al., 2001). Both Chisel and ANF were significantly downregulated (Fig. 6I-L). Another NKX2.5 downstream target, HOP (Chen et al., 2002; Shin et al., 2002), which is a novel homeodomain protein that serves a negative feedback for NKX2.5 function, remained normal in the mutant hearts at E9.5 (Fig. 6M,N). In addition, cardiogenic transcriptional factor eHand also remained normal in BMP10-deficient hearts, while dHand was slightly downregulated (data not shown). These finds suggested that NKX2.5 and MEF2C were regulated by BMP10.

BMP10 is able to promote embryonic cardiomyocyte growth and rescue BMP10-deficient hearts in culture

To further analyze the biological activity of BMP10, we generated BMP10-expressing NIH3T3 cells using a retroviral gene delivery system (Fig. 7A, part a). The expression of BMP10 in these cells was confirmed by northern blot analysis (data not shown). Using BMP10-expressing cells as feeders, we established a co-culture system in which freshly isolated wild-type embryonic cardiomyocytes were laid on top of mitomycin C pre-treated (non-mitotic) BMP10-expressing cells or control cells. BMP10-expressing feeder cells maintained a higher [^{3}H]thymidine labeling index in embryonic cardiomyocytes after 48 hours of co-culture compared with control co-cultures (Fig. 7A, part b), indicating that BMP10 has growth-promoting activity for embryonic cardiomyocytes. This growth-promoting activity of BMP10 was also confirmed using BMP10-conditioned media in both cell culture and organ culture (Fig. 7B).

When we applied BMP10-conditioned media to isolated BMP10-deficient hearts in culture, we found BMP10-conditioned media rescued BMP10-deficient hearts (Fig. 7B,

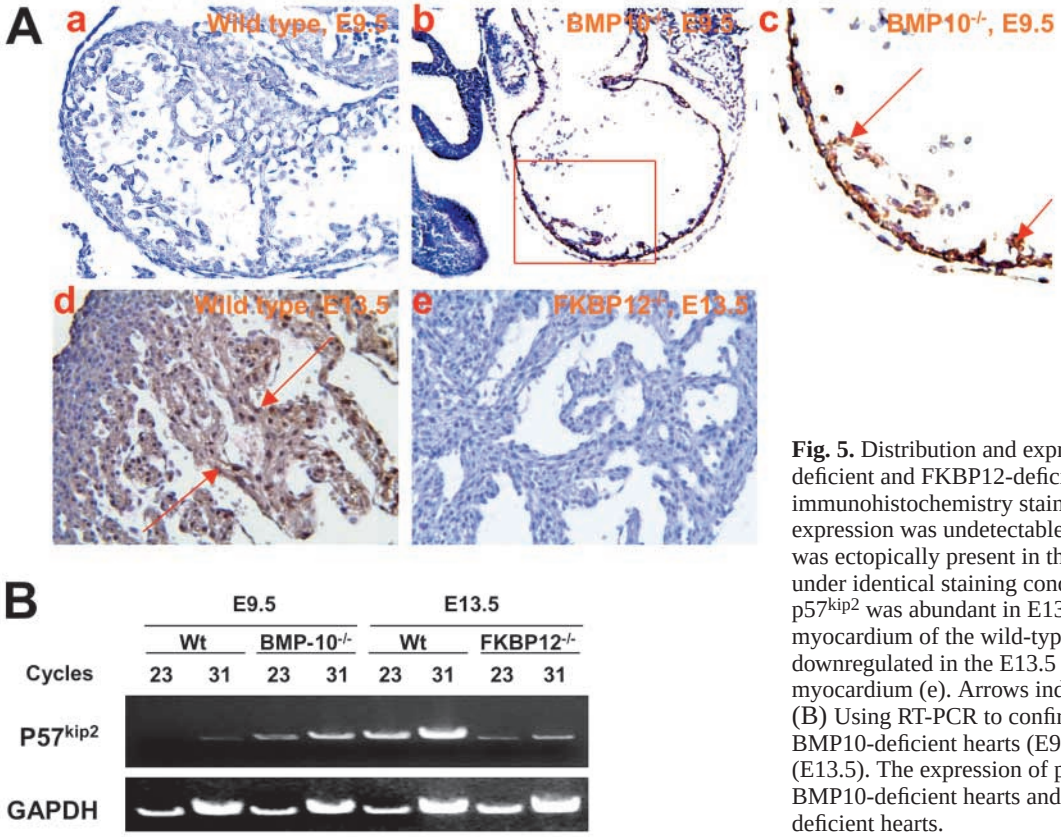

Fig. 5. Distribution and expression of $p57^{kip2}$ in BMP10-deficient and FKBP12-deficient hearts using immunohistochemistry staining. (A) At E9.5, $p57^{kip2}$ expression was undetectable in the wild-type heart (a) but was ectopically present in the BMP10-deficient heart (b,c) under identical staining conditions. The expression of $p57^{kip2}$ was abundant in E13.5 ventricular trabecular myocardium of the wild-type heart (d) but was significantly downregulated in the E13.5 FKBP12-deficient trabecular myocardium (e). Arrows indicate areas of positive staining. (B) Using RT-PCR to confirm the mRNA level of $p57^{kip2}$ in BMP10-deficient hearts (E9.5) and FKBP12-deficient hearts (E13.5). The expression of p57kip2 was upregulated in BMP10-deficient hearts and downregulated in FKBP12-deficient hearts.

part b). The rescued BMP10-deficient hearts displayed significant improvements in cardiac size, [^{3}H]thymidine labeling (Fig. 7B, part d, and Fig. 7C), and cardiac performance as measured by the improved heart rate (Fig. 7D). This experiment further delineated the essential role for BMP10 in cardiac development.

Mutant mice deficient in neuregulin or its receptor ErbB developed severe defects in ventricular trabeculation (Meyer and Birchmeier, 1995; Gassmann et al., 1995; Lee et al., 1995). To determine if the strong effect of BMP10 on myocardium was via a neuregulin–ErbB-mediated pathway, we cultured BMP10-deficient hearts in the neuregulin (NRG-1)-containing media (Rentschler et al., 2002). Unlike BMP10-conditioned medium, NRG-1 medium was not able to rescue the growth-deficiency phenotype of BMP10-deficient hearts (data not shown). This observation suggested that BMP10 was either downstream of, or irrelevant to, the neuregulin–ErbB-mediated pathway.

Importantly, when E9.5 mutant hearts were cultured in BMP10-conditioned media, both NKX2.5 (Fig. 8A) and MEF2C (data not shown) expression was restored, and $p57^{kip2}$ expression was significantly downregulated in these rescued hearts (Fig. 8B). This observation further indicated the close relationship between BMP10 and cardiogenic transcriptional factors NKX2.5 and MEF2C and cell cycle regulator $p57^{kip2}$.

In summary, our studies demonstrated that the presence of BMP10 in the developing ventricle at E8.75-E9.0 is crucial in maintaining the proliferative activity of the embryonic cardiomyocytes by preventing premature activation of the negative cell cycle regulator $p57^{kip2}$ and in maintaining the required expression level of two very important cardiogenic factors, NKX2.5 and MEF2C, in the developing heart at mid-gestation (Fig. 9).

Discussion

The importance of BMP10 to cardiac development is reflected by its temporal and spatial pattern of expression. It is known that cardiac cell cycle withdraw is associated with ventricular chamber maturation, myocyte terminal differentiation and lineage specification. The fact that trabecular myocytes have lower proliferative activity than that of compact wall suggests that trabecular myocytes initiate the process of terminal differentiation earlier (Rumyantsev, 1991; Icardo, 1984). In this regard, cardiac growth and chamber maturation has to be regulated by a temporally and spatially controlled process and a balance between proliferation and terminal differentiation. During trabeculation (E9.0-13.5 in the mouse), trabecular myocardium is required to expand in order to generate sufficient numbers of myocytes to contribute to future ventricular septum, papillary muscles and conductive system cells; at the same time, these cells are also required to reduce proliferative activity for terminal differentiation and lineage specification. Although it is still not clear about the identities of negative growth signals, $p57^{kip2}$, a negative cell cycle regulator, is one of the intracellular candidates and is initially found in trabecular myocardium at E10.5 (Kochilas et al., 1999). Interestingly, cardiac defects have not been reported in $p57^{kip2}$-deficient mice (Zhang et al., 1997; Yan et al., 1997), suggesting that there are other negative regulators involved, in a cooperative way with $p57^{kip2}$, in the cardiac cell cycle withdraw and terminal differentiation. In fact, there is evidence

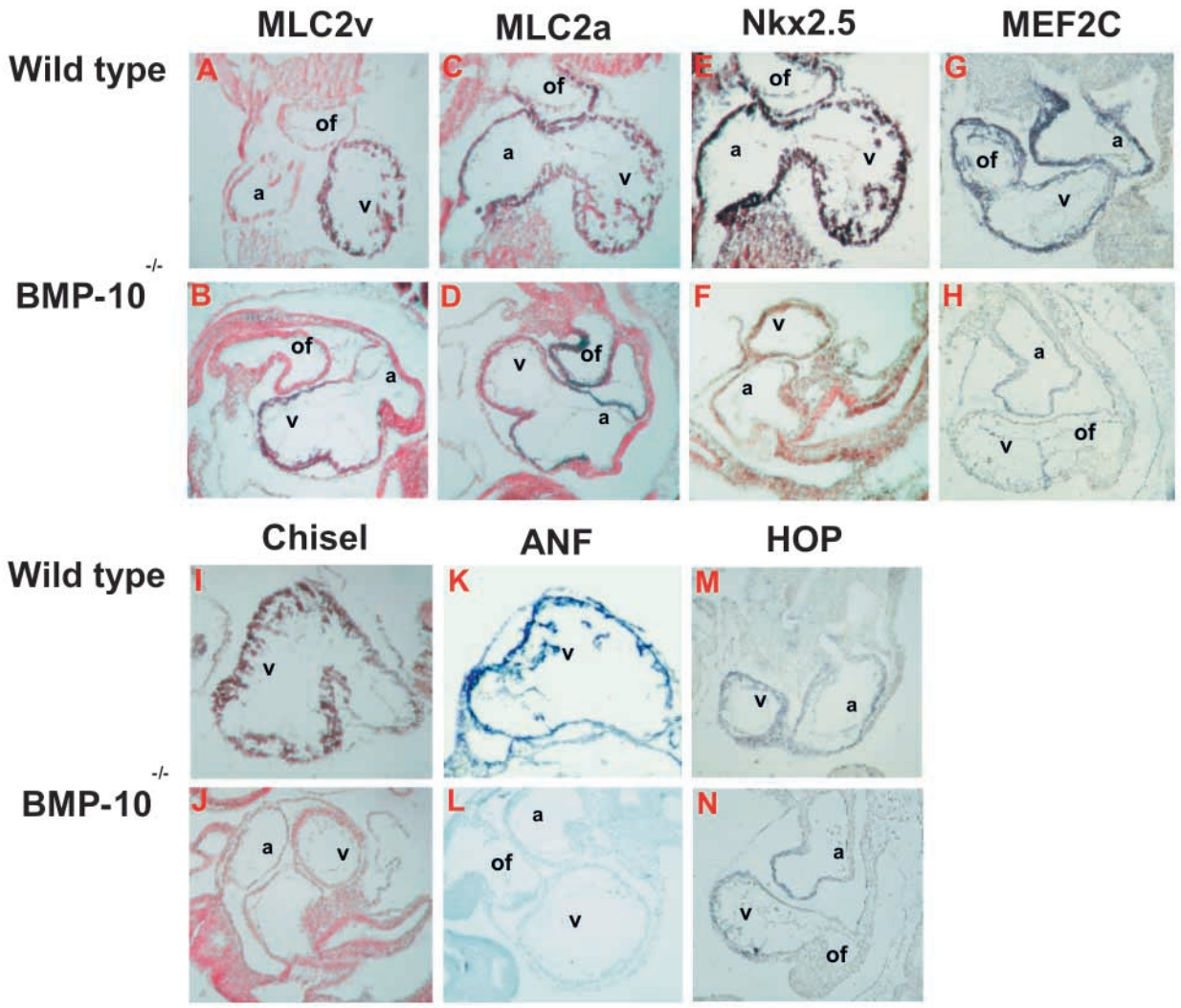

Fig. 6. Analysis of cardiac markers in BMP10-deficient hearts. Using in-situ hybridization to analyze the expression of cardiac markers at E9.5. The cardiac chamber markers MLC2v (A,B) and MLC2a (C,D) were not altered in the BMP10-deficient hearts, suggesting that cardiac patterning and chamber specification are normal in the BMP10-deficient heart. Cardiogenic transcription factors NKX2.5 (E,F) and MEF2C (G,H) were significantly downregulated at E9.5 in the BMP10-deficient hearts. The expression of Chisel (I,J) and ANF (K,L) was also reduced in the BMP10-deficient heart, while the expression of HOP (M,N) remained at a similar level in the BMP10-deficient heart compared with the control heart. a, atrium; v, ventricle; of, outflow tract.

that $p57^{kip2}$ and other negative cell cycle regulators (e.g. $p21^{cip1}$ and $p27^{kip1}$) cooperate to regulate cell cycle exit and cell differentiation of skeletal muscle cells, lens fiber cells and placenta trophoblasts (Zhang et al., 1998; Zhang et al., 1999). Our data support the suggestion that BMP10 provides a positive growth signal for cardiomyocytes that antagonizes negative regulators such as $p57^{kip2}$. Perturbation of this balance would lead to either cardiac hyperplasia and hypertrabeculation and noncompaction (e.g. elevation of BMP10 expression in FKBP12-deficient hearts) or the cardiac hypoplasia seen in BMP10-deficient hearts.

Another important finding in our studies is that BMP10 was specifically required to maintain the expression level of cardiogenic transcription factors NKX2.5 and MEF2C during mid-gestation. Both NKX2.5 and MEF2C have been shown to be critical for cardiac patterning in the early phase of cardiogenesis (for a review, see Harvey et al., 1999; Black and Olson, 1999). BMP10-deficient hearts have normal cardiac patterning, which is consistent with the normal expression of NKX2.5 and MEF2C before E9.0. However, the rapid downregulation of NKX2.5 and MEF2C in E9.5 mutant hearts may help to explain the severely impaired cardiac function seen in BMP10-deficient hearts, since many of the NKX2.5 and MEF2C downstream gene products are crucial for cardiac function.

A related observation is that the downregulation of NKX2.5 and MEF2C is not restricted to the ventricular chamber in which BMP10 is expressed. In fact, in a similar way to other BMPs, BMP10 is a secreted peptide that can function as an autocrine and paracrine growth and differentiation signal, which would lead to a broader effect during cardiac development. The lack of seeded mesenchymal cells in endocardial cushions in BMP10-deficient hearts and the relative normal cushion structure in rescued hearts suggest that

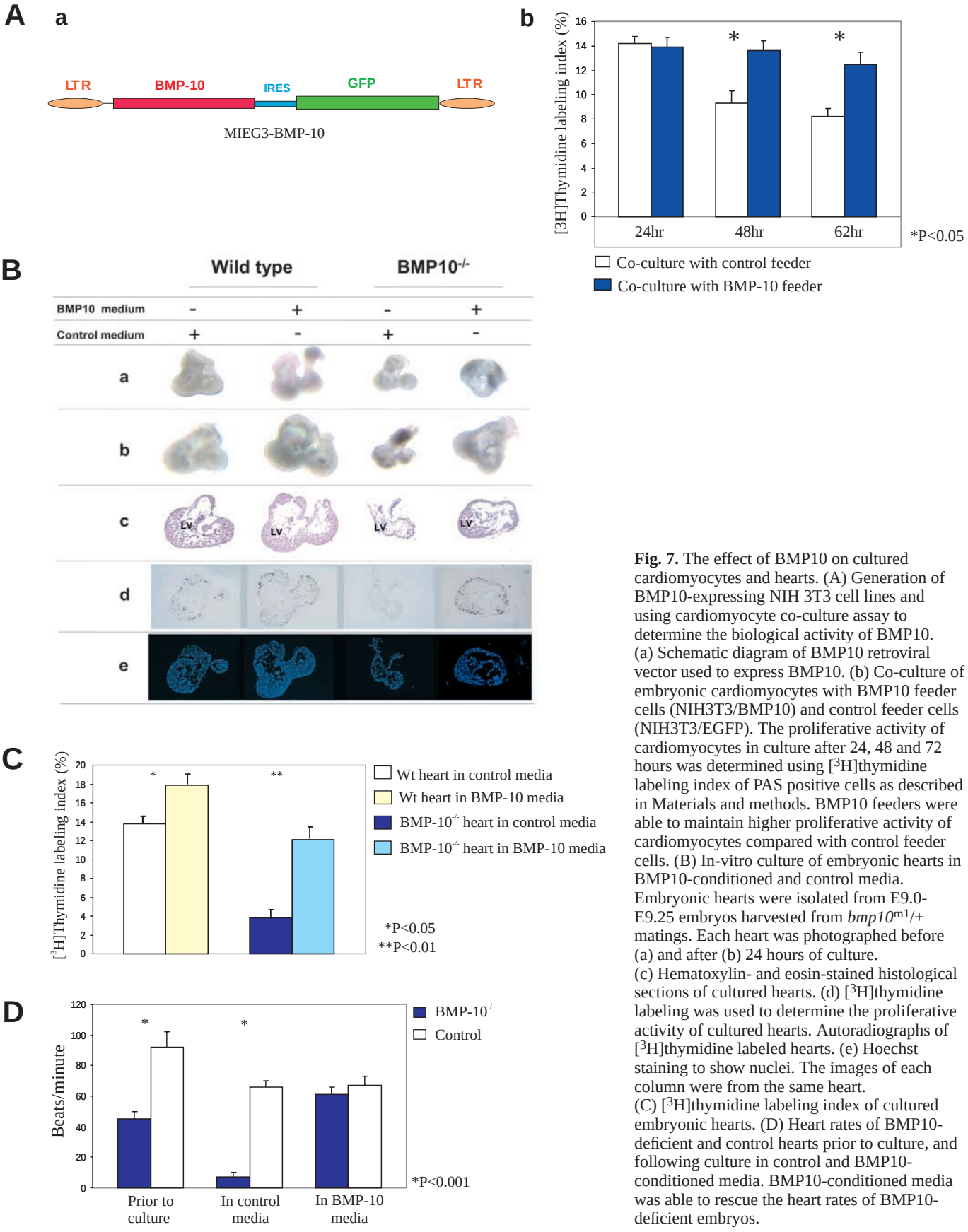

Fig. 7. The effect of BMP10 on cultured cardiomyocytes and hearts. (A) Generation of BMP10-expressing NIH 3T3 cell lines and using cardiomyocyte co-culture assay to determine the biological activity of BMP10. (a) Schematic diagram of BMP10 retroviral vector used to express BMP10. (b) Co-culture of embryonic cardiomyocytes with BMP10 feeder cells (NIH3T3/BMP10) and control feeder cells (NIH3T3/EGFP). The proliferative activity of cardiomyocytes in culture after 24, 48 and 72 hours was determined using [^{3}H]thymidine labeling index of PAS positive cells as described in Materials and methods. BMP10 feeders were able to maintain higher proliferative activity of cardiomyocytes compared with control feeder cells. (B) In-vitro culture of embryonic hearts in BMP10-conditioned and control media. Embryonic hearts were isolated from E9.0-E9.25 embryos harvested from *bmp10*^{m1}/+ matings. Each heart was photographed before (a) and after (b) 24 hours of culture. (c) Hematoxylin- and eosin-stained histological sections of cultured hearts. (d) [^{3}H]thymidine labeling was used to determine the proliferative activity of cultured hearts. Autoradiographs of [^{3}H]thymidine labeled hearts. (e) Hoechst staining to show nuclei. The images of each column were from the same heart. (C) [^{3}H]thymidine labeling index of cultured embryonic hearts. (D) Heart rates of BMP10-deficient and control hearts prior to culture, and following culture in control and BMP10-conditioned media. BMP10-conditioned media was able to rescue the heart rates of BMP10-deficient embryos.

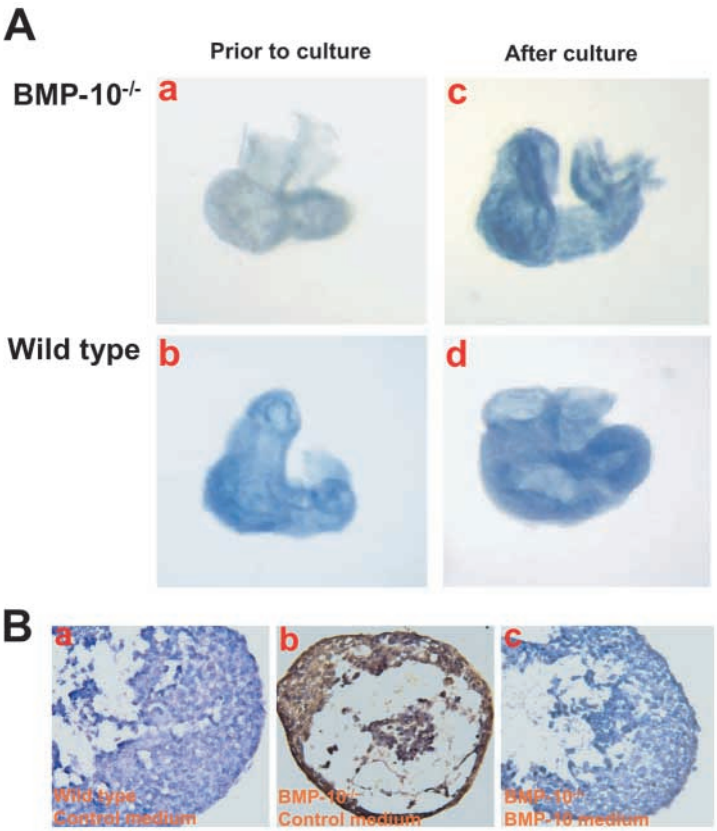

Fig. 8. BMP10-conditioned medium restored the normal genetic program in BMP10-deficient hearts. (A) Whole-mount in-situ hybridization of NKX2.5 expression in cultured embryonic hearts. Embryonic hearts were isolated at E9.0 and cultured in BMP10-conditioned media overnight. Prior to the culture, the BMP10-deficient hearts (n=3) (a) had a significantly lower NKX2.5 expression than the littermate control hearts (n=3) (b). After culture, the BMP10-deficient hearts (n=4) (c) had restored NKX2.5 expression. (d) Littermate control heart (n=3) cultured in BMP10-conditioned medium. (B) Immunohistological staining of $p57^{kip2}$ expression in cultured embryonic hearts. Embryonic hearts were isolated at E9.0 and cultured in BMP10-conditioned media or control medium overnight. (a) Wild-type hearts cultured in control medium (n=6). (b) BMP10-deficient hearts cultured in control medium (n=4). (c) BMP10-deficient hearts cultured in BMP10-conditioned medium (n=4). The expression of $p57^{kip2}$ in mutant hearts cultured in BMP10-conditioned medium was significantly downregulated when compared with the mutant hearts cultured in control medium.

BMP10 is able to contribute to the epithelial–mesenchymal transformation, a key step in endocardial cushion development. However, we cannot yet exclude the likelihood that the cushion defect in BMP10 mutant heart is secondary to severely impaired cardiac growth in vivo.

In addition to the cardiac-specific BMP10, other BMPs (e.g. BMP-2, -4, -5, -6 and -7) and TGFβ family members and receptors (for a review, see Schneider et al., 2003), which have much wider expression patterns during embryonic development, are also found in the developing heart. These BMPs appear to form an important network that controls several crucial morphogenetic events during cardiac development. Obviously, these BMPs are not able to compensate for the loss of BMP10 in vivo. Probably, this is partially due to their differences in temporal and spatial pattern of expression and partially due to their differences in ligand-receptor specificity. During cardiac development, BMP2/4 is more restricted to the myocardium adjacent to the endocardial cushion region (Nakajima et al., 2000). BMP-5, -6 and -7 have overlapping expression patterns and redundant functions in cardiac development (Solloway and Robertson, 1999; Kim et al., 2001). Mice deficient in both BMP-6 and BMP-7 develop outflow tract and valvo-septation anomalies (Kim et al., 2001), while mice deficient in both BMP-5 and BMP-7 have defects in cardiac looping and ventricular chamber formation (Solloway and Robertson, 1999). In our on-going rescue experiments using different BMPs (e.g. BMP-2, -4, -5 and -6, and TGFβ-1), we clearly observed the differences in their ability to rescue the BMP10-deficient hearts in culture (data not shown). This finding suggests a complicated BMP-receptor network in the developing heart. It is consistent with recent data in cardiac conditional knockout of type I receptor for BMP (Alk3) (Gaussin et al., 2002). Cardiac myocyte-specific deletion of Alk3 leads to major defects in endocardial cushion and ventricular wall but has very little effect on cardiac trabeculation. BMP10 expression is also normal in these mutant mice. Interestingly, NKX2.5 and other cardiogenic transcription factors are not altered in Alk3 mutant hearts, suggesting that Alk3 is not the receptor mediating BMP10 signaling.

Recently, analysis of the NKX2.5 promoter showed that NKX2.5 expression in both early and late cardiac development is mediated by multiple conserved Smad binding sites (Liberatore et al., 2002; Lien et al., 2002). This finding further suggests that BMP signaling is required beyond the initial step of cardiogenic induction. Previously, BMP2/4 has been shown to mediate cardiac induction via activation of NKX2.5 in chick embryos at an early stage (Schultheiss et al., 1997) (for a

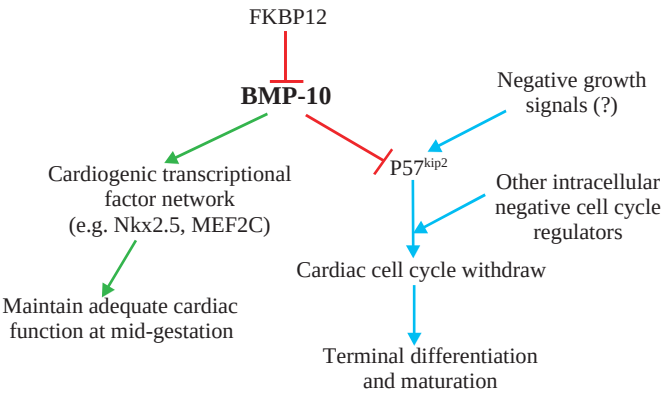

Fig. 9. A model for the modulation of cardiac growth and function by BMP10 during mid-gestation. FKBP12 negatively regulates BMP10 possibly via its interaction to type I receptor for BMP10. BMP10 has double biological activities: (1) it prevents the premature activation and/or antagonizes the activity of negative cell cycle regulators such as $p57^{kip2}$; (2) it maintains cardiac function by regulating the level of expression of several key cardiogenic transcriptional factors during mid-gestation.

review, see Srivastava and Olson, 2000). Our data supported the observation from NKX2.5 promoter analysis. BMP10 is a strong candidate that is responsible for maintaining the expression of NKX2.5 during mid-gestation, possibly via a Smad-NKX2.5 pathway.

Our studies have demonstrated an important genetic pathway that regulates ventricular trabeculation and chamber maturation. The regulation of BMP10 expression may be an important mechanism for normal cardiac trabecular growth and compaction in mice. Genetic investigation of human patients with noncompaction myocardial defects may demonstrate a role for BMP10 in this pathological condition as well.

Note added in proof

A recent related study by Pashmforoush et al. (Pashmforoush et al., 2004) has indicated that *Nkx2.5* can act as a negative-feedback regulator of BMP10 expression at later developmental stages. Mutant mice with a late onset cardiomyocyte-specific *Nkx2.5* null mutation, generated via a conditional cre/loxP knockout strategy, have an abnormal myocardium with increased ventricular trabeculation. Significantly, BMP10 expression is ectopically upregulated in these conditional *Nkx2.5*-deficient hearts. These findings further support a role for BMP10 in ventricular maturation and underscore the deleterious effects of abnormal BMP10 regulation during the pathogenesis of ventricular non-compaction in murine models. Further studies will be required to determine the link between BMP10 and the etiology of ventricular non-compaction in humans.

We wish to thank Dr Shaolian Jing and Mr William Carter of Indiana University Mouse Core for their superb assistance in generating BMP10 knockout mice, Dr Loren Field for his generous support and valuable discussion and Drs Michael Rubart-Von Der Lohe, Kishore Pasumarthi and Hisako Nakajima for their generous help in this study. This study was supported in part by National Institute of Health HL70259 (W.S.), HL63196 (M.Y.), HLOK04071 (L.H.), HL60714 (S.J.C.), Showalter Research Foundation (W.S. and L.H.), Muscular Dystrophy Association (W.S.), the Riley Children's Foundation (W.S., M.Y., L.H.).

References

Andree, B., Duprez, D., Vorbusch, B., Arnold, H. H. and Brand, T. (1998). BMP-2 induces ectopic expression of cardiac lineage markers and interferes with somite formation in chicken embryos. *Mech. Dev.* **70**, 119-131.

Bao, S., Shen, X., Shen, K., Liu, Y. and Wang, X. F. (1998). The mammalian Rad24 homologous to yeast *Saccharomyces cerevisiae* Rad24 and *Schizosaccharomyces pombe* Rad17 is involved in DNA damage checkpoint. *Cell Growth Differ.* **9**, 961-967.

Barron, M., Gao, M. and Lough, J. (2000). Requirement for BMP and FGF signaling during cardiogenic induction in non-precardiac mesoderm is specific, transient, and cooperative. *Dev. Dyn.* **218**, 383-393.

Black, B. L. and Olson, E. N. (1999). Control of cardiac development by the MEF2 family of transcription factors. In *Heart Development* (ed. R. P. Harvey and N. Rosenthal), pp. 131-142. San Diego: Academic Press.

Chen, F., Kook, H., Milewski, R., Gitler, A. D., Lu, M. M., Nazarian, R., Schnepp, R., Jen, K., Biben, C., Runke, G., Mackay, J. P., Novotny, J., Schwatz, R. J., Harvey, R. P., Mullins, M. C. and Epstein, J. A. (2002). Hop is an unusual homeobox gene that modulates cardiac development. *Cell* **110**, 713-723.

Conway, S. J., Henderson, D. J. and Copp, A. J. (1997). Pax3 is required for cardiac neural crest migration in the mouse: evidence from the splotch (Sp2h) mutant. *Development* **124**, 505-514.

Ducy, P. and Karsenty, G. (2000). The family of bone morphogenetic proteins. *Kidney International* **57**, 2207-2214.

Dumont, D. J., Gradwohl, G., Fong, G. H., Puri, M. C., Gertsenstein, M., Auerbach, A. and Breitman, M. L. (1994). Dominant-negative and targeted null mutations in the endothelial receptor tyrosine kinase, tek, reveal a critical role in vasculogenesis of the embryo. *Genes Dev.* **8**, 1897-1909.

Durocher, D., Chen, C-Y., Ardati, A., Schwartz, R. J. and Nemer, M. (1996). The atrial natriuretic factor promoter is a downstream target for Nkx-2.5 in the myocardium. *Mol. Cell Biol.* **16**, 4648-4655.

Dusek, J., Ostadal, B. and Duskova, M. (1975). Postnatal persistence of spongy myocardium with embryonic blood supply. *Arch. Pathol.* **99**, 312-317.

Ferrara, N., Carver-Moore, K., Chen, H., Dowd, M., Lu, L., O'Shea, K. S., Powell-Braxton, L., Hillan, K. J. and Moore, M. W. (1996). Heterozygous embryonic lethality induced by targeted inactivation of the VEGF gene. *Nature* **380**, 439-442.

Franco, D. and Icardo, J. M. (2001). Molecular characterization of the ventricular conduction system in the developing mouse heart: topographical correlation in normal and congenitally malformed hearts. *Cardiovasc. Res.* **49**, 417-429.

Franco, D., deBoer, P. A., deGier-de Vries, C., Lamers, W. H. and Moorman, A. F. (2001). Methods on in situ hybridization, immunohistochemistry and beta-galactosidase reporter gene detection. *Eur. J. Morphol.* **39**, 169-191.

Gassmann, M., Casagranda, F., Oriori, A. Simon, H., Lai C. and Klein, R. and Lemek, G. (1995). Aberrant neural and cardiac development in mice lacking the ErbB4 neuregulin receptor. *Nature* **378**, 390-394.

Gaussin, V., Van de Putte, T., Mishina, Y., Hanks, M. C., Zwijsen, A., Huylebroeck, D., Behringer, R. R. and Schneider, M. D. (2002). Endocardial cushion and myocardial defects after cardiac myocyte-specific conditional deletion of the bone morphogenetic protein receptor ALK3. *Proc. Natl. Acad. Sci. USA* **99**, 2878-2883.

Haneline, L. S., Li, X., Ciccone, S. L. M., Hong, P., Yang, Y., Lee, S-H., Orazi, A., Srour, E. F. and Clapp, D. W. (2003). Retroviral-mediated expression of recombinant Fancc enhances the repopulating ability of *Fancc–/–* hematopoietic stem cells and decreases the risk of clonal evolution. *Blood* **101**, 1299-1307.

Harvey, R. P., Biben, C. and Elliott, D. A. (1999). Transcriptional control and pattern formation in the developing vertebrate heart: studies on NK-2 class homeodomain factors. In *Heart Development* (ed. R. P. Harvey and N. Rosenthal), pp. 111-129. San Diego: Academic Press.

Icardo, J. M. (1984). The growing heart: an anatomical perspective. In *Growth of the Heart in Health and Disease* (ed. R. Zak), pp. 41-79. New York: Raven Press.

Ichida, F., Tsubata, S., Bowles, K. R., Haneda, N., Uese, K., Miyawaki, T., Dreyer, W. J., Messina, J., Li, H., Bowles, N. E. and Towbin, J. A. (2001). Novel gene mutations in patients with left ventricular noncompaction or Bath Syndrome. *Circulation* **103**, 1256-1263.

Kim, R. Y., Robertson, E. J. and Solloway, M. J. (2001). Bmp6 and Bmp7 are required for cushion formation and septation in the developing mouse heart. *Dev. Biol.* **235**, 449-466.

Kochilas, L. K., Li, J., Jin, F., Buck, C. A. and Epstein, J. A. (1999). P57kip2 expression is enhanced during mid-cardiac murine development and is restricted to trabecular myocardium. *Pediatr. Res.* **45**, 635-642.

Lee, K. F., Simon, H., Chen, H., Bates, B., Hung, M. C. and Hauser, C. (1995). Requirement for neuregulin receptor ErbB2 in neural and cardiac development. *Nature* **378**, 394-398.

Liberatore, C. M., Searcy-Schrick, R. D., Vincent, E. B. and Yutzey, K. E. (2002). Nkx-2.5 gene induction in mice is mediated by a Smad concensus regulatory region. *Dev. Biol.* **244**, 243-256.

Lien, C-L., McAnally, J., Richardson, J. A. and Olson, E. N. (2002). Cardiac-specific activity of an NKX2-5 enhancer requires an evolutionarily conserved Smad binding site. *Dev. Biol.* **244**, 257-266.

Massague, J. and Chen, Y. G. (2000). Controlling TGF-beta signaling. *Genes Dev.* **14**, 627-644.

Meyer, D. and Birchmeier, C. (1995). Multiple essential functions of neuregulin in development. *Nature* **378**, 386-390.

Millauer, B., Wizigmann-Voos, S., Schnurch, H., Martinez, R., Moller, N. P., Risau, W. and Ullrich, A. (1993). High affinity VEGF binding and developmental expression suggest Flk-1 as a major regulator of vasculogenesis and angiogenesis. *Cell* **72**, 835-846.

Moorman, A. F. M. and Lamers, W. H. (1999). Development of the conduction system of the vertebrate heart. In *Heart Development*. (ed. R. P. Harvey and N. Rosenthal), pp. 195-207. San Diego: Academic Press.

Nakajima, Y., Yamagishi, T., Hokari, S. and Nakamura, H. (2000). Mechanisms involved in valvuloseptal endocardial cushion formation in early cardiogenesis: roles of transforming growth factor (TGF)-beta and bone morphogenetic protein (BMP). *Anat. Rec.* **258**, 119-127.

Nakayama, T., Cui, Y. and Christian, J. L. (2000). Regulation of BMP/Dpp signaling during embryonic development. *Cell Mol. Life Sci.* **57**, 943-956.

Neuhaus, H., Rosen, V. and Thies, R. S. (1999). Heart specific expression of mouse BMP-10 a novel member of the TGF-β superfamily. *Mech. Dev.* **80**, 181-184.

Palmer, S., Groves, N., Schindeler, A., Yeoh, T., Biben, C., Wang, C-C., Sparrow, D. B., Barnett, L., Jemkins, N. A., Copeland, N. G., Koentgen, F., Mohum, T. and Harvey, R. P. (2001). The small muscle-specific protein Csl modifies cell shape and promotes myocyte fusion in an insulin-like growth factor 1-dependent manner. *J. Cell Biol.* **153**, 985-997.

Pashmforoush, M., Lu, J. T., Chen, H., St Amand, T., Kondo, R., Pradervand, S., Evans, S. M., Clark, R., Feramisco, J. R., Giles, W., Ho, S. Y., Benson, W. D., Silberbach, M., Shou, W. and Chien, K. R. (2004). Defects in Nkx 2.5 pathways for ventricular myocytes lineage specification leads to progressive cardiomyopathy and atrioventricular heart block. *Cell* (in press).

Rentschler, S., Zander, J., Meyers, K., France, D., Levine, R., Porter, G., Rivkees, S. A., Morley, G. E. and Fishman, G. I. (2002). Neuregulin-1 promotes formation of the murine cardiac conduction system. *Proc. Natl. Acad. Sci. USA* **99**, 10464-10469.

Rumyantsev, P. P. (1991). Growth and hyperplasia of cardiac muscle cells. In *Soviet Medical Reviews Supplement series* (ed. B. M. Carlson), pp. 12-36. London: Harwood Academic Publishers.

Schneider, M. D., Gaussin, V. and Lyons, K. M. (2003). BMP signals for cardiac morphogenesis. *Cytokine Growth Factor Rev.* **14**, 1-4.

Schott, J. J., Benson, D. W., Basson, C. T., Pease, W., Silberbach, G. M., Moak, J. P., Maron, B. J., Seidman, C. E. and Seidman, J. G. (1998). Congenital heart disease caused by mutations in the transcription factor NKX2-5. *Science* **281**, 108-111.

Schultheiss, T. M., Burch, J. B. and Lassar, A. B. (1997). A role for bone morphogenetic proteins in the induction of cardiac myogenesis. *Genes Dev.* **11**, 451-462.

Shin, C. H., Liu, Z-P., Passier, R., Zhang, C-L., Wang, D-Z., Harris, T. M., Yamagishi, H., Richardson, J. A., Childs, G. and Olson, E. N. (2002). Modulation of cardiac growth and development by HOP, an unusual homeodomain protein. *Cell* **110**, 725-735.

Shou, W., Aghdasi, B., Armstrong, D. L., Guo, Q., Bao, S., Charng, M-J., Mathews, L. S., Schneider, M. D., Hamilton, S. L. and Matzuk, M. M. (1998). Cardiac defects and altered ryanodine receptor function in mice lacking FKBP12. *Nature* **391**, 489-492.

Solloway, M. J. and Robertson, E. J. (1999). Early embryonic lethality in Bmp5; Bmp7 double mutant mice suggests functional redundancy within the 60A subgroup. *Development* **126**, 1753-1768.

Srivastava, D. and Olson, E. N. (2000). A genetic blueprint for cardiac development. *Nature* **407**, 221-226.

Suri, C., Jones, P. F., Patan, S., Bartunkova, S., Maisonpierre, P. C., Davis, S., Sato, T. N. and Yancopoulos, G. D. (1996). Requisite role of angiopoietin-1, a ligand for the TIE2 receptor, during embryonic angiogenesis. *Cell* **87**, 1171-1180.

Wang, T., Donahoe, P. K. and Zervos, A. S. (1994). Specific interaction of type 1 receptor of the TGF-β family with the immunophilin FKBP-12. *Science* **265**, 674-676.

Wang, T., Li, B.-Y., Danielson, P. D., Shah, P. C., Rockwell, S., Lechleider, R. J., Martin, J., Manganaro, T. and Donahoe, P. K. (1996).The immunophilin FKBP12 functions as a common inhibitor of the TGFβ family type 1 receptors. *Cell* **86**, 435-444.

Winnier, G. E., Kume, T., Deng, K., Rogers, R., Bundy, J., Raines, C., Walter, M. A., Hogan, B. L. and Conway, S. (1999). Roles for the winged helix transcription factors MF1 and MFH1 in cardiovascular development revealed by nonalletic noncomplementation of null alleles. *Dev. Biol.* **213**, 418-431.

Yan, Y., Frisen, J., Lee, M. H., Massague, J. and Barbacid, M. (1997). Ablation of the CDK inhibitor p57kip2 results in increased apoptosis and delayed differentiation during development. *Genes Dev.* **11**, 973-983.

Zhang, P., Liegeois, N. J., Wong, C., Finegold, M., Hou, H., Thompson, J. C., Silverman, A., Harper, J. W., DePinho, R. A. and Elledge, S. J. (1997). Altered cell differentiation and proliferation in mice lacking p57kip2 indicates a role in Beckwith-Wiedemann syndrome. *Nature* **387**, 151-158.

Zhang, P., Wong, C., DePinho, R. A., Harper, J. W and Elledge, S. J. (1998). Cooperation between the Cdk inhibitors p21kip1 and p57kip2 in the control of tissue growth and development. *Genes Dev.* **12**, 3162-3167.

Zhang, P., Wong, C., Liu, D., Finegold, M., Harper, J. W. and Elledge, S. J. (1999). p21cip1 and p57kip2 control muscle differentiation at the myogenin step. *Genes Dev.* **13**, 213-224.